Development of a Hovering Robot System for Calamity Observation

M.S. Kang, S. Park, H.G. Lee, D.H. Won, and T.J. Kim

Division of Applied Robot Technology(DART)
Korea Institute of Industrial Technology(KITECH), Korea
(Tel : +82-31-400-3988; E-mail: {wowmecha, sdpark, leehg, daehee, re94}@kitech.re.kr)

Abstract: A QRT(Quad-Rotor Type) hovering robot system is developed for quick detection and observation of the circumstances under calamity environment such as indoor fire spots. The UAV(Unmanned Aerial Vehicle) is equipped with four propellers driven by each electric motor, an embedded controller using a DSP, INS(Inertial Navigation System) using 3-axis rate gyros, a CCD camera with wireless communication transmitter for observation, and an ultrasonic range sensor for height control. The developed hovering robot shows stable flying performances under the adoption of RIC(Robust Internal-loop Compensator) based disturbance compensation and the vision based localization method. The UAV can also avoid obstacles using eight IR and four ultrasonic range sensors. The VTOL(Vertical Take-Off and Landing) flying object flies into indoor fire spots and sends the images captured by the CCD camera to the operator. This kind of small-sized UAV can be widely used in various calamity observation fields without danger of human beings under harmful environment.

Keywords: QRT(Quad-Rotor Type), UAV(Unmanned Aerial Vehicle), VTOL(Vertical Take-Off and Landing), Hovering, INS(Inertial Navigation System), RIC(Robust Internal-loop Compensator), Vision based localization

1. INTRODUCTION

Recently the merit and application of small-sized UAVs(Unmanned Aerial Vehicles) have been being increased explosively as the design and control technologies for the small flying objects have been combined with various high technologies. Small-sized UAVs have wider operation range and better mobility in the environment with many obstacles than on-the-ground mobile robots. Further, small-sized UAVs are much cheaper and safer in dangerous tasks than piloted aircrafts. These kinds of UAVs can be widely applied in various tasks from calamity observation such as wood and building fires, meteorological observation, patrol, and spraying agricultural chemicals to military purpose such as reconnaissance, monitoring, and communication.

Small-sized UAVs are classified into two categories, fixed and rotary wing types. The rotary wing type UAVs are more advantageous than the fixed wing type ones in the sense of VTOL(Vertical Take-off and Landing), omni-directional flying, and hovering performances, and can be divided into QRTs(Quad-Rotor Types), same axis reverse rotation types, and helicopter types as their shapes. QRTs have the simplest mechanical structures among them, and that is the reason why the QRT is considered in this study as a flying platform for calamity observation such as indoor fire spots etc.

QRT small-sized UAVs with various shape and size have been developed for commercial and research purposes, and some models are being sold as RC(Radio Control) toys. Autonomous QRT UAVs equipped with high technology sensors are also being developed for special purposes, and researches for analysis and control of the flying robots are being done vigorously. V. Mistler, A. Benellegue and N.K. M'Sirdi derived the dynamic model for a four rotors helicopters, and developed a dynamic feedback controller[1]. P. McKerrow obtained the dynamic model for theoretical analysis of a draganflyer[2]. A. Mokhtari and A. Benellegue obtained a nonlinear dynamic model of a QRT UAV for state variable control based on Euler angle and an open loop position state observer, emphasized attitude control rather than the translational motion of the UAV[3]. P. Castilo, R. Loranzo and A. Daul performed autonomous take-off, hovering and landing control of a QRT UAV by synthesizing a controller using the Lagrangian model based on the Lyapunov analysis[4]. S. Bouabdallah, P. Murrieri and R. Siegwart performed the design, dynamic modelling, sensing and control of an indoor micro QRT UAV[5].

Flight control methods utilizing vision systems are also studied. E. Altuğ, J.P. Ostrowski, and R. Mahony proposed a visual feedback control method of a QRT UAV using a camera equipped on the UAV as the main sensor for attitude estimation[6]. T. Hamel, R. Mahony and A. Chriette proposed a vision based visual servo controller for performing trajectory tracking tasks of under-actuated systems like QRT UAVs[7]. T. Hanel and R. Mahony proposed a vision based controller which performs visual servo control by positioning a camera onto a fixed target for the hovering of a QRT UAV[8].

In this study a QRT hovering robot system is developed for calamity observation under harmful environment. The dynamics of the UAV is derived, and a vision based localization and RIC based flight control methods for the developed QRT UAV are introduced. The performance of the proposed control scheme is verified through experiments. Section 2 shows the basic structure and the dynamics of the UAV. The RIC(Robust Internal-loop Compensator) based flight control algorithms and the vision based localization schemes are given in section 3 and 4, respectively. Section 5 shows the experimental setup and experimental results

2. DYNAMIC MODELING OF A QRT UAV

2.1 Basic Structure of a QRT UAV

The QRT UAV considered in this study is an under-actuated system which has four rotors driven by each motor mounted at the end of a crossing body frame as shown in Fig. 1. The rotors generate thrust forces($\boldsymbol{F}_i$) perpendicular the plane of the rotors and counter torques($\boldsymbol{\tau}_i$) with respect to the center of each rotor according to the speed(Ω_i) of each motor. Generally, The QRT UAVs have four rotors in cross configuration. The two pairs of rotors(1,3) and (2,4) turn in opposite directions. When all four rotors spin at the same rate, the moments will cancel and equilibrium can be achieved.

The merit of QRT UAVs lies in their simple mechanical structures. However, QRT UAVs have some demerits in their low payload to weight ratio and difficulties in operation. The research efforts for the QRT UAVs, therefore, are mainly focused on 1) increasing their payload to weight ratio by improving load capacity the UAVs and/or by miniaturizing on board components such as sensors and controllers, and 2) developing control algorithms for autonomous flight and improved mobility of the UAVs.

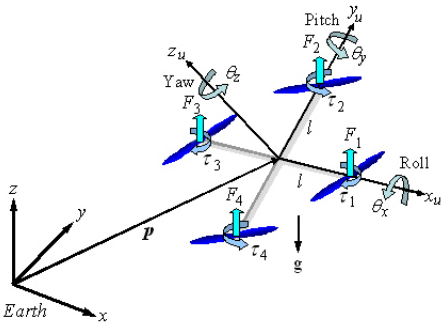

Fig. 1 The coordinate system if a QRT UAV

2.2 Dynamic Modeling of a QRT UAV

Fig. 1 shows the coordinate system of a QRT UAV. When the thrust forces Fi and counter torques i are applied to the UAV fixed on the moving coordinate system, the equations of motion of the UAV at inertial coordinate frame is given as follows.

$$\begin{bmatrix} m & 0 & 0 \\ 0 & m & 0 \\ 0 & 0 & m \end{bmatrix}\begin{pmatrix} \ddot{x} \\ \ddot{y} \\ \ddot{z} \end{pmatrix} + \begin{pmatrix} 0 \\ 0 \\ mg \end{pmatrix} + \mathbf{K}_{\mathbf{f}}\begin{pmatrix} \dot{x} \\ \dot{y} \\ \dot{z} \end{pmatrix} = \mathbf{R}(\theta)\mathbf{F}\,, \qquad (1)$$

$$\begin{bmatrix} I_x & 0 & 0 \\ 0 & I_y & 0 \\ 0 & 0 & I_z \end{bmatrix}\begin{pmatrix} \ddot{\theta}_x \\ \ddot{\theta}_y \\ \ddot{\theta}_z \end{pmatrix} + \mathbf{K}_{\mathbf{m}}\begin{pmatrix} \dot{\theta}_x \\ \dot{\theta}_y \\ \dot{\theta}_z \end{pmatrix} = \mathbf{M}\,, \qquad (2)$$

where m and I_i are the mass and mass moment of inertia of the UAV, respectively, and $\mathbf{K_f}$ and $\mathbf{K_m}$ are the resistant coefficients by air with respect to translational and rotational motion of the UAV. $\mathbf{R}(\theta)$ is the rotational matrix given by

$$\mathbf{R}(\theta) = \begin{pmatrix} c\theta_y c\theta_z & s\theta_x s\theta_y c\theta_z - c\theta_x s & c\theta_x s\theta_y c\theta_z + s\theta_x s\theta_z \\ c\theta_y s\theta_z & s\theta_x s\theta_y s\theta_z + c\theta_x c & c\theta_x s\theta_y s\theta_z - s\theta_x c\theta_z \\ -s\theta_y & s\theta_x c\theta_y & c\theta_x c\theta_y \end{pmatrix} \qquad (3)$$

where $s\theta_i = \sin\theta_i$, $c\theta_i = \cos\theta_i$. The external force **F** and the moment **M** applied to the UAV are given as

$$\mathbf{F} = \begin{bmatrix} 0 & 0 & 0 & 0 \\ 0 & 0 & 0 & 0 \\ 1 & 1 & 1 & 1 \end{bmatrix}\begin{pmatrix} F_1 \\ F_2 \\ F_3 \\ F_4 \end{pmatrix}, \quad \text{and}$$

$$\mathbf{M} = \begin{bmatrix} 0 & l & 0 & -l \\ -l & 0 & l & 0 \\ -\lambda & \lambda & -\lambda & \lambda \end{bmatrix}\begin{pmatrix} F_1 \\ F_2 \\ F_3 \\ F_4 \end{pmatrix} \qquad (4)$$

respectively, where l is the length between the center of the moving coordinate fixed to the UAV and the center of rotation of each rotor, and λ is a proportional constant between F_i and τ_i. The thrust force F_i can be defined as follows.

$$F_i = b\Omega^2 \qquad (5)$$

Where b is the thrust factor. And, representation of the moment **M** is as follows.

$$\mathbf{M} = \begin{bmatrix} bl(\Omega_2^{\,2} - \Omega_4^{\,2}) \\ bl(-\Omega_1^{\,2} + \Omega_3^{\,2}) \\ b\lambda(-\Omega_1^{\,2} + \Omega_2^{\,2} - \Omega_3^{\,2} + \Omega_4^{\,2}) \end{bmatrix} \qquad (6)$$

If the UAV is assumed to move at low speed, the resistant coefficients $\mathbf{K_f}$ and $\mathbf{K_m}$ in (1) and (2) can be negligible, and substitution of (3), (4) and (6) into (1) and (2) gives the resultant equations of motion as follows

$$\begin{pmatrix} \ddot{x} \\ \ddot{y} \\ \ddot{z} \\ \ddot{\theta}_x \\ \ddot{\theta}_y \\ \ddot{\theta}_z \end{pmatrix} = \begin{bmatrix} (\cos\theta_x \sin\theta_y \cos\theta_z + \sin\theta_x \sin\theta_z)u_1 \\ (\cos\theta_x \sin\theta_y \sin\theta_z + \sin\theta_x \cos\theta_z)u_2 \\ (\cos\theta_x \cos\theta_y)u_1 - g \\ u_2 \\ u_3 \\ u_4 \end{bmatrix} \qquad (7)$$

where $u_i (i = 1, 2, 3, 4)$ are control inputs satisfying the equations of motion of the UAV as follows:

$$
\begin{aligned}
u_1 &= b(\Omega_1^{\,2} + \Omega_2^{\,2} + \Omega_3^{\,2} + \Omega_4^{\,2})/m \\
u_2 &= bl(\Omega_2^{\,2} - \Omega_4^{\,2})/I_x \\
u_3 &= bl(-\Omega_1^{\,2} + \Omega_3^{\,2})/I_y \\
u_4 &= b\lambda(-\Omega_1^{\,2} + \Omega_2^{\,2} - \Omega_3^{\,2} + \Omega_4^{\,2})/I_z
\end{aligned} \tag{8}
$$

QRT UAVs have four controllable DOF as seen in (8), but they can move in three dimensional space with six DOF satisfying two dynamic constraints, i.e., one thrust force F_i is not compatible with one directional movement. In this study the altitude, and three attitude angles, roll, pitch and yaw, are chosen as four controllable DOF. Controller design for the system with dynamics in (7) is described in the following section.

3. CONTROLLER DESIGN

3.1 Basic Structure of the Controller

Fig. 2 shows the basic structure for the flight control of the UAV. Equation (8) can be rewritten as

$$\mathbf{U} = \mathbf{S} \cdot \mathbf{D} \cdot \Omega\,, \tag{9}$$

where $\mathbf{U} = [u_1,\ u_2,\ u_3,\ u_4]^T$ are the control inputs of the system, $\Omega = [\Omega_1^{\,2},\ \Omega_2^{\,2},\ \Omega_3^{\,2},\ \Omega_4^{\,2}]^T$ are the thrust forces of DC motors, and **S** and **D** are proportional and distribution matrices, respectively, given as follows:

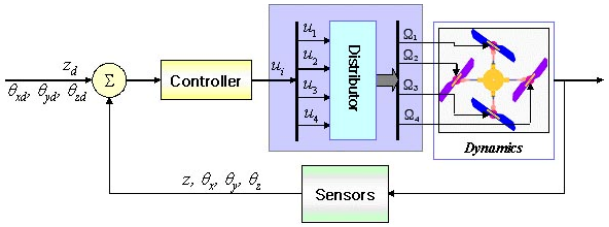

Fig. 2 Basic structure of the controller for the UAV.

$$
\mathbf{S} = \begin{bmatrix} b/m & 0 & 0 & 0 \\ 0 & b/I_x & 0 & 0 \\ 0 & 0 & b/I_y & 0 \\ 0 & 0 & 0 & b\lambda/I_z \end{bmatrix},\quad \mathbf{D} = \begin{bmatrix} 1 & 1 & 1 & 1 \\ 0 & 1 & 0 & -1 \\ -1 & 0 & 1 & 0 \\ -1 & 1 & -1 & 1 \end{bmatrix} \tag{10}
$$

From (9), the rotor speeds Ω_i applied to each DC motor are distributed from the control inputs u_i as

$$\Omega = \mathbf{D}^{-1} \cdot \mathbf{S}^{-1} \cdot \mathbf{U}\,. \tag{11}$$

3.2 Control Algorithm

3.2.1 Basic Control Control Algorithm

The control algorithms for the altitude and attitude, roll, pitch and yaw, of the UAV are designed based on PID controllers as shown in Fig. 3. The control input u_1 for controlling the altitude z of the UAV with respect to the reference input z_d is designed as

$$u_1 = K_{p1}(z_d - z) + K_{d1}\frac{(z_d - z)}{dt} + K_{i1}\int_0^t (z_d - z)d\tau\,. \tag{12}$$

The control inputs u_j (j =2, 3, 4) for controlling the attitude θ_k ($k = x, y, z$) of the UAV with respect to the reference inputs θ_{kd} are designed given, respectively as:

$$u_j = K_{pj}(\theta_{kd} - \theta_k) - K_{dj}\dot{\theta}_k + K_{ij}\int_0^t (\theta_{kd} - \theta_k)d\tau - \bar{u}_j\,. \tag{13}$$

$\bar{u}_j$ are the PD control inputs for avoiding obstacles in roll and pitch axis given as:

$$
\begin{aligned}
\bar{u}_2 &= \left\{K_{pr}(d_{rd} - d_r) + K_{dr}\dot{d}_r\right\}U(d_{rd} - d_r) \\
&\quad - \left\{K_{pl}(d_{ld} - d_l) + K_{dl}\dot{d}_l\right\}U(d_{ld} - d_l) \\
\bar{u}_3 &= \left\{K_{pb}(d_{bd} - d_b) + K_{db}\dot{d}_b\right\}U(d_{bd} - d_b) \\
&\quad - \left\{K_{pf}(d_{fd} - d_f) + K_{df}\dot{d}_f\right\}U(d_{fd} - d_f) \\
\bar{u}_4 &= 0
\end{aligned} \tag{14}
$$

where d_{md} (m = f, b, l, r) are reference distances for avoiding obstacles to forward, backward, left, and right direction, and d_m (m = f, b, l, r) are detected distances of obstacles to the four direction. $U(d_{md} - d_m)$ (m = f, b, l, r) are step functions as follows:

$$
U(d_{md} - d_m) = \begin{cases} 1 & \text{for } d_{md} < d_m \\ 0 & \text{for } d_{md} > d_m \end{cases} \quad (m = f, b, l, r) \tag{15}
$$

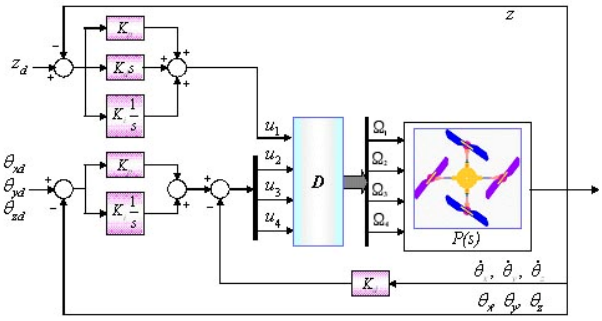

Fig. 3 PID controller for controlling the altitude and attitude of the UAV.

3.2.2 RIC Based Disturbance Compensation

The control algorithms (12) and (13) control the altitude and attitude of the UAV using sensor signals. The flight performance of the UAV, however, is not good in real flight because of the sensor noise and disturbances. The RIC based control algorithm, as shown in Fig. 4, controls the response of the plant $P(s)$ to follow that of the model plant $P_m(s)$ even

though disturbances d_{ex} and sensor noise ξ are applied to the plant[9, 10].

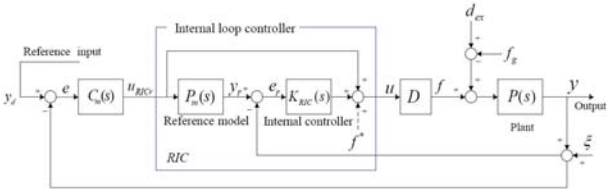

Fig. 4 RIC supplemented disturbance compensation controller.

RIC based disturbance compensator can be used both for altitude and attitude control in the same way. In the cases the reference plant models are given in the form of force-mass and inertia-moment dynamic models without friction, respectively as

$$P_{zm}(s) = \frac{1}{m_{zm}s^2}, \quad P_{\theta m}(s) = \frac{1}{I_{zm}s^2}, \tag{16}$$

where m_{zm} and I_{km} (k = x, y, z) are the mass and mass moment of inertia in each direction of the UAV, respectively.

The external-loop compensator $C_{zm}(s)$ for altitude control, for instance, are given like PD controller as follows:

$$C_{zm}(s) = K_{pz} + K_{dz}s, \tag{17}$$

where K_{pz} and K_{dz} are P- and D-gain of the external-loop compensator, respectively. The output of the external-loop compensator, i.e., the reference input of RIC is given as

$$f_{zr} = C_{zm}(s)e_z, \tag{18}$$

and the output of the reference model z_r becomes

$$z_r = P_m(s)\cdot f_{zr} = \frac{1}{m_{zm}s^2}(K_{pz}e_z + K_{dz}e_z s). \tag{19}$$

In Fig.4

$$z_r = z_d + e_{zr} - e_z, \tag{20}$$

since $e_{zr} = z_r - (z+\xi)$ and $e_z = z_d - (z+\xi)$. Thus, from (19) and (20), the model following error becomes

$$e_{zr} = e_z - z_d + \frac{1}{m_{zm}s^2}(K_{pz}e_z + K_{dz}e_z s). \tag{21}$$

From (18) and (21) the RIC control input, therefore, is given as follows:

$$\begin{aligned} f_z &= f_{zr} + K^z_{RIC}(s)e_{zr} \\ &= K_{pz}e_z + K_{dz}e_z s \\ &\quad + K^z_{RIC}(s)\left(-(z+\xi) + \frac{K_{pz}}{m_{zm}s^2}e_z + \frac{K_{dz}}{m_{zm}s^2}e_z\right) + f^*_z \end{aligned} \tag{22}$$

Where $K^z_{RIC}(s) = K^z_p + K^z_d s + K^z_i \frac{1}{s}$ and $f^*_{zz} = m_{zm}g$. The procedures for obtaining the RIC control input for attitude control are the same with that for altitude control except that $f^*_\theta = 0$.

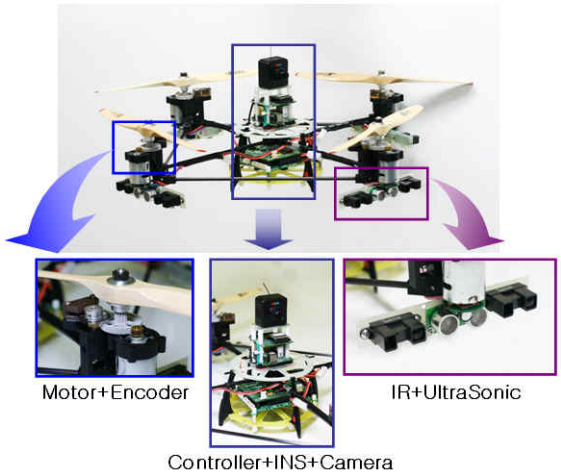

Fig.5 The developed QRT small sized UAV for indoor calamity observation

4. EXPERIMENTS AND RESULTS

4.1 Experimental Setup

Fig. 5 shows the fabricated QRT UAV for the purpose of calamity observation in indoor environment. The UAV has four rotors driven by each DC motor mounted at each end of a crossing body frame. The UAV is also equipped with an INS(Inertial Navigation System) composed of three rate gyros and three accelerometer, eight IR and four ultrasonic range sensors for obstacle detection, and one additional ultrasonic sensor for altitude measuring. A CCD camera with wireless RF transmitter is mounted on the top of the UAV for the observation task. Table 1 gives the specification of the developed UAV. Fig.6 shows the schematic view of the embedded controller using a TMS320F2812 DSP controller.

Table 1 Specification of the developed UAV.

Item	Specification	Item	Specification
Diameter	700mm	Payload	Max. 1.5kg
Height	150mm	Rotor Dia.	11"
Weight	11.1kg (Except batteries)	Rotor Pitch	6"

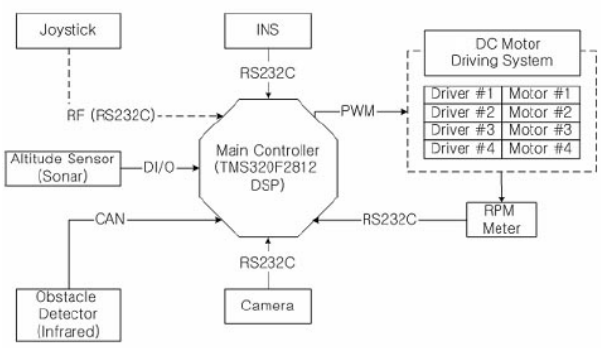

Fig. 6 The schematic view of the embedded controller

4.2 Vision Based Localization

Fig. 7 shows the scheme of the vision based localization. As the payload of the UAV is limited, a red and a green LED markers are attached at the bottom of the UAV, and a CCD camera is put on the ground. The CCD camera gets the image of the LED markers, and the image processor analyze the color distribution of the markers, extract the center of each marker and fine the position and orientation of the markers as shown in Fig. 8[11]. It takes 25ms for the image processing, and 5ms for serial communication.

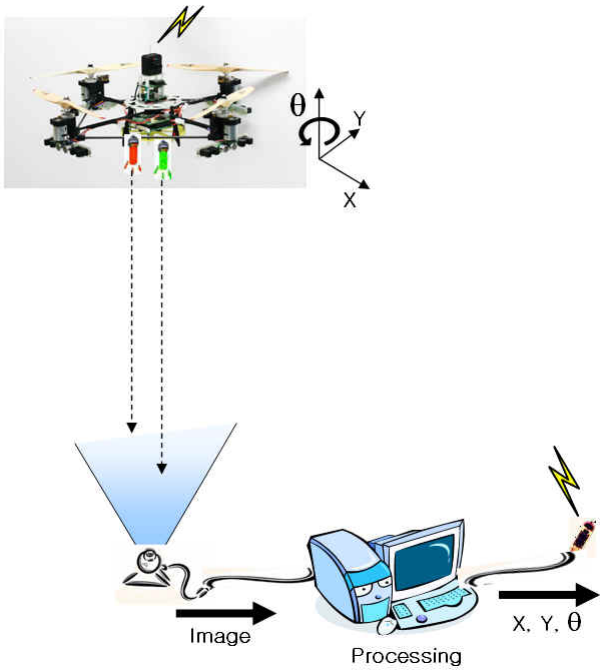

Fig. 7 The scheme of the vision based localization.

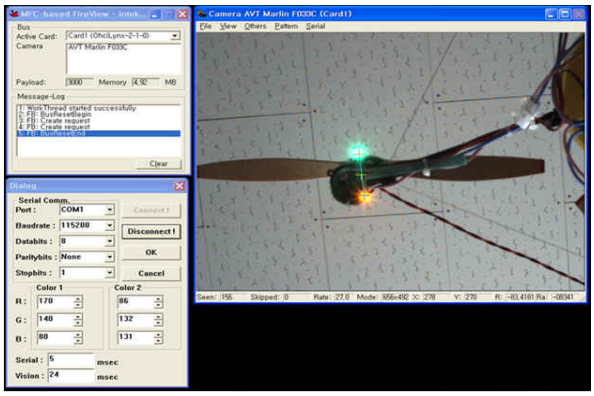

Fig. 8 The result of the vision based localization.

4.3 Experiments and Results

Hovering and attitude control experiments are carried out using the developed UAV, and Fig. 9 shows the experimental results. The left column of Fig. 9 (a) shows roll, pitch, and yaw rates (up to down) and the right column for roll, pitch, and yaw angles during hovering. Fig. 9 (b), (c), and (d) show three angle rates and angles for pitch, roll, and yaw control. The results show that the proposed algorithm for both the altitude and attitude control of the UAV works well.

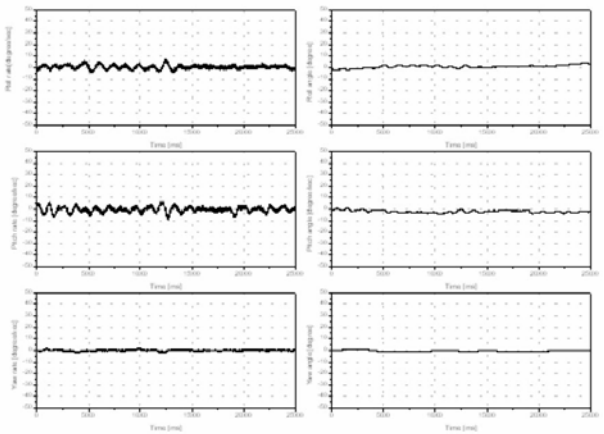

(a) Experimental results during hovering of the UAV.

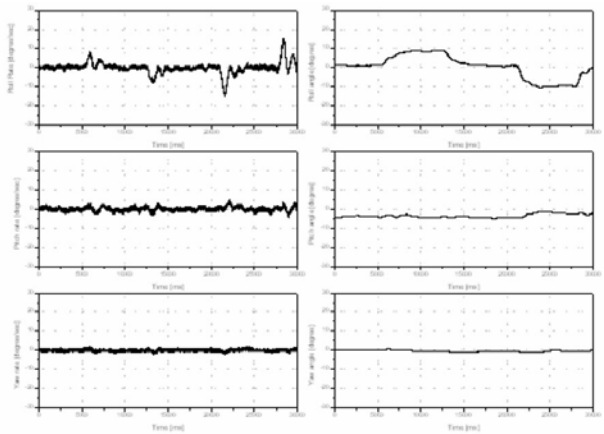

(b) Experimental results for desired roll angle of the UAV = ±10 deg.

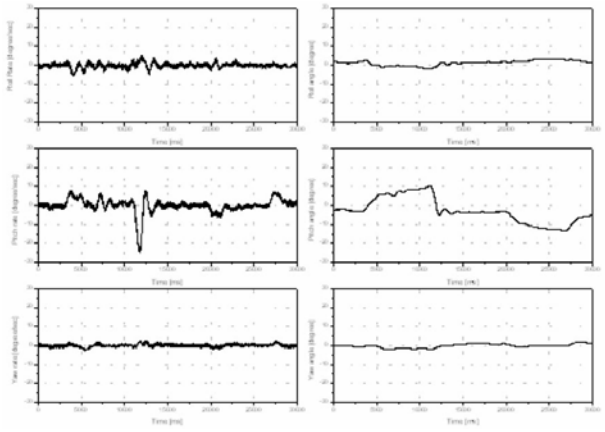

(c) Experimental results for desired pitch angle of the UAV = ±10 deg.

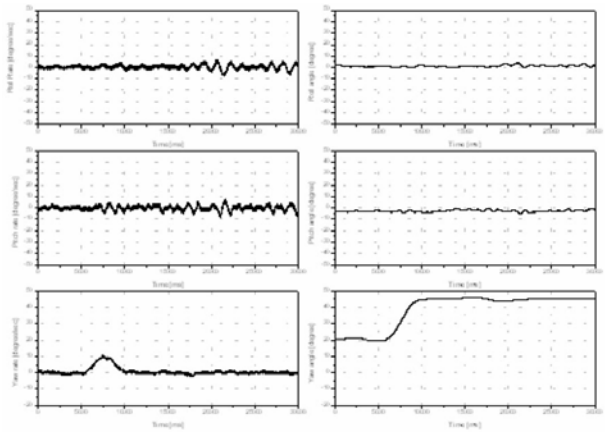

(d) Experimental results for desired yaw angle of the UAV = +45 deg.

Fig. 9 The experimental results for hovering and attitude control of the developed UAV.

5. CONCLUDING REMARKS

In this study, a QRT UAV is developed for calamity observation in indoor environment. The hovering robot captures the image of targets under harmful environment and sends the image to the operator on safe site. The developed hovering robot shows stable flying performances by adopting the RIC based disturbance compensation and the vision based localization method. The UAV can also avoid obstacles using eight IR and four ultrasonic range sensors. Further study will be focused on the improvement of payload to weight ratio and the enhancement of autonomous flight performance of the QRT UAV.

REFERENCES

[1] V. Mistler, A. Benallegue and N.K. M'Sirdi, "Exact linearization and noninteracting control of a 4 rotors helicopter via dynamic feedback" *Proceedings of IEEE Intrnaltional Workshop on Robot and Human Interactive Communication*, 2001, pp. 586~593.

[2] P. McKerrow, "Modeling the Draganflyer for-rotor helicopter," *Proceedings of the 2004 IEEE International Conference on Robotics & Automation*, New Orleans, LA, 2004, pp. 3596~3601.

[3] A. Mokhtari and A. Benallegue, "Dynamic Feedback Controller of Euler Angles and Wind parameters estimation for a Quadrotor Unmanned Aerial Vehicle," *Proceedings of the 2004 IEEE International Conference on Robotics & Automation*, New Orleans, LA, 2004, pp. 2359~2366.

[4] P. Catillo, R. Loranzo and A. Dzul, "Stabilization of a mini-rotorcraft having four rotors," *Proceedings of IEEE/RSJ International Conference on Intelligent Robots and Systems*, Sendai, Japan, 2004, pp. 2693~2698.

[5] S. Bouabdallah, P. Murrieri, and R. Siegwart, "Design and Control of an Indoor Micro Quadrotor," *Proceedings of the 2004 IEEE International Conference on Robotics & Automation*, New Orleans, LA, 2004, pp. 4393~4398.

[6] E. Altuğ, J.P. Ostrowski, and R. Mahony, "Control of a Quadrotor Helicopter Using Visual Feedback," *Proceedings of the 2002 IEEE International Conference on Robotics & Automation*, Washington, DC, 2002, pp. 72~77.

[7] T. Hamel, R. Mahony, and A. Chriette, "Visual servo trajectory tracking for a four rotor VTOL aerial vehicle," *Proceedings of the 2002 IEEE International Conference on Robotics & Automation*, Washington, DC, 2002, pp. 2781~2786.

[8] T. Hamel and R. Mahony, "Pure 2D Visual Servo control for a class of under-actuated dynamic system," *Proceedings of the 2002 IEEE International Conference on Robotics & Automation*, New Orleans, LA, 2004, pp. 2229~2235.

[9] B.K. Kim, S. Park, W.K. Chung, and Y. Youm, "Robust Motion Controller Design for Flexible XY Positioning System," *Journal of Control, Automation, and Systems Engineering, Vol. 9, No. 1*, 2003, pp. 82~89.

[10] B.K. Kim and W.K. Chung, "Advanced Disturbance Observer Design for Mechanical Positioning Systems," *IEEE Transactions on Industrial Electronics, Vol. 50, No. 6, 2003*, pp. 1207~1216.

[11] K.-J. Yoon, G.-J. Jang, S.-H. Kim, and I.-S. Kweon, "Color Landmark Based Self-Localization for Indoor Mobile Robots," *Journal of Control, Automation, and Systems Engineering, Vol. 7, No. 9*, 2001, pp. 749~757.